Influence of PPH dendrimers' surface functions on the activation of human monocytes: A study of their interactions with pure lipid model systems

F. Ielasi, Jérémy Le Dall, Alexandra Perez Anes, Séverine Fruchon, A.-M. Caminade, Rémy Poupot, Cédric-Olivier Turrin, Muriel Blanzat

Journal Name

ARTICLE

Influence of PPH dendrimers' surface functions on the activation of human monocytes. Study of their interactions with pure lipid model systems

Received 00th January 20xx,
Accepted 00th January 20xx

DOI: 10.1039/x0xx00000x

www.rsc.org/

F. Ielasi, †,a J. Ledall, †,b,c,d A. Perez Anes,a,b,c S. Fruchon,d A.-M. Caminade,b,c R. Poupot,*,d C.-O. Turrin*,b,c and M. Blanzat*,a

The influence of the surface function on the interactions between Poly(PhosphorHydrazone) PPH dendrimers and human monocytes is discussed on the basis of complementary biological and physicochemical studies on membrane models (monolayers and multi lamellar vesicles). The studies were performed on both an active and non-toxic acid phosphonic capped dendrimer and a non-active but toxic acid carboxylic capped one. On the one hand, comparative studies of the behaviour of DPPC monolayers in the presence or not of PPH dendrimers in the subphase showed differences on the phase transitions, highlighting interactions between both dendrimers and phospholipid monolayers, with a larger incidence for acid carboxylic capped dendrimer (negative control), validating its cellular toxicity. On the other hand, comparative biological studies (activation of human monocytes and binding of fluorescent dendrimers on human monocytes) show the pre-eminence of acid phosphonic capped dendrimers towards specific binding and subsequent activation of human monocytes.

Introduction

Dendrimers,[1] perfectly defined highly branched macromolecules with adjustable multivalent surfaces, are each day more represented in the field of nanosciences and nanomedicine.[2] In this respect, Poly(PhosphorHydrazone) (PPH) dendrimers[3] offer a high polyvalence for the surface functionalization[4] which allowed the exploration of their multivalent interactions[5] with biological entities like viruses[6] or DNA,[7] and nanomaterials.[8] For instance we have demonstrated the crucial importance of the nature of polyanionic PPH dendrimers surface functions on their HIV1 inhibition properties,[9] and similar observations were made with PPH dendrimers capable of expanding *ex vivo* human NK (natural killer) cells.[10]

Recently, we have shown that PPH dendrimers capped with phosphonic acid derivatives are able to activate human monocytes according to an anti-inflammatory pathway[11] which is accompanied by immuno-modulations like the specific inhibition of T-CD4+ lymphocytes[12] and a strong anti-osteoclastic effect.[13] These results open exciting perspectives for alternative strategies for the treatment of chronic inflammatory diseases, like rheumatoid arthritis[13] and multiple sclerosis.[14] These innovative biological properties have been shown to be highly dependent on several structural parameters of the dendrimers, like their size and generation, and also related to the local density[15] and to the nature of the surface functions.[16] Recently, we have demonstrated for the first time that the three dimensional conformation induced by the entire internal scaffold is crucial for the bioactivity of dendrimers.[17] Among PPH dendrimers, only those capped with azabisphosphonic groups promoted a significant activation of monocytes in culture.[18] An exhaustive screening led to the definition of dendrimer **D-1** (Figure 1) as a lead compound.

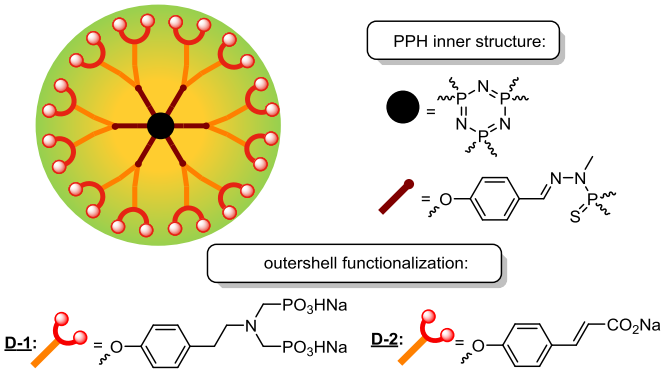

Figure 1. Structure of dendrimer **D-1** and dendrimer **D-2**.

a. Laboratoire IMRCP, UMR 5623 CNRS, Université Toulouse 3
118 route de Narbonne, F-31062 Toulouse (France)
Fax: +33(0)561-558-155
E-mail: blanzat@chimie.ups-tlse.fr.
b. Laboratoire de Chimie de Coordination du CNRS, UPR 8241
205 route de Narbonne, BP 44099, F-31077 Toulouse cedex 04
Fax: +33(0)561-553-003
E-mail: turrin@lcc-toulouse.fr
c. Université de Toulouse, UPS, INPT, LCC, F-31077 Toulouse
d. Centre de Physiopathologie de Toulouse-Purpan, INSERM 1043, CNRS 5282, université de Toulouse ; F-31300 Toulouse
Fax:+33(0)562-744-558
E-mail: remy.poupot@inserm.fr
† These authors contributed equally to this work

Please do not adjust margins

A recent study performed on the biological behaviour of these anti-inflammatory PPH dendrimers has proved that their interactions with cell membranes also depend on the nature of the surface function. The azabisphosphonate-terminated PPH dendrimer **D-1** has shown to interact both specifically and non-specifically with human monocytes, whereas only non-specific interactions were observed with an isosteric analogue having twelve azabiscarboxylate groups.[20] These findings brought a first crucial answer on how PPH dendrimer **D-1** activates monocytes. Specific receptor(s), that have to be isolated, are clearly involved in this process.

Surprisingly, during the extensive dendrimer screening, cytotoxicity experiments indicated that only one specific dendrimer, the carboxylate-capped PPH dendrimer **D-2**, is highly cytotoxic for human Peripheral Blood Mononuclear Cells (PBMC). This toxicity was observed even at low concentrations (0.2 to 200 µM), whereas no toxicity was observed for dendrimer **D-1** (figure 2) and its isosteric analogue previously described.[19,20]

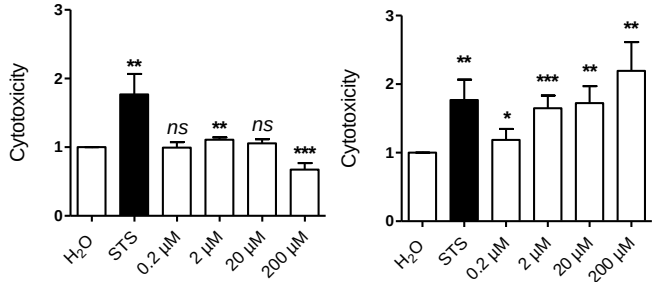

Figure 2. Toxicity of dendrimers on PBMCs. Toxicity on 5 donors was evaluated by a CellTox™ Green Cytotoxicity Assay after 24 hours of treatment with dendrimers **D-1** (left) or **D-2** (right) at concentrations from 0.2 µM to 200 µM. Staurosporin (STS, black bars) was used as a positive control of cytotoxicity. Cytotoxicity is quantified as the ratio of the numbers of dead cells in the condition and in the H_2O control Data are represented as mean ± SD from five independent donors. *p<0.05, **p<0.01, ***p<0.001 (one-tailed paired *t*-test *vs* H_2O).

In order to rationalise the activation properties and the cytotoxicity of both dendrimer structures, the physicochemical behaviour of compound **D-1** has been compared to the one of carboxylated dendrimer **D-2**. We have previously shown that the anti-inflammatory activation of monocytes with PPH dendrimers responds to structural considerations that take into account all the key topological features of dendrimers like surface function,[16,18] nature of the scaffold,[17] size[18] and local density of surface function.[15] For instance, we have already shown that the number of charge is not a key parameters, as other bis-methylene phosphonates endgroups[16] were found to be less active that the one grafted on dendrimer **D-1**. Our interest on dendrimer 2 is related to its unexpected cytotoxic behaviour mentioned above. In this regard, the interactions between PPH dendrimers **D-1** or **D-2** and phospholipidic monolayers, used as two-dimensional models of lipidic membranes,[21,22] have been explored to tentatively explain the different biological behaviours from a physicochemical point of view. In a second step, the interactions of these dendrimers with phospholipidic bilayers[23] have been studied by calorimetry[24] to highlight the possible bilayer's modifications that could contribute to the cytotoxicity of carboxylate-capped PPH dendrimer **D-2**. In a last step, biological experiments on human monocytes have been performed to correlate the physicochemical findings with the interaction properties of both dendrimers.

Results and Discussion

Obviously, interactions between dendrimers and cell-surface are highly dependent on the nature of the dendrimer surface. The latter having itself a great influence on the physicochemical properties of the macromolecules, we have first determined the critical aggregation concentration (CAC) of the dendrimers, both in aqueous and saline physiological solutions using the pendant drop method. It should be noted that both carboxylic and phosphonic acid terminated dendrimer are ionized at the pH of the studies. Results show that the CAC values found for **D-1** in water or in physiological PBS solution are close to 37 mM (Figure 3), that is 2000-fold the concentration at which the dendrimer is able to activate monocyte populations ex vivo (20 µM).[18] This result indicates that despite self-association properties at water-air interfaces, compound **D-1** exerts its biological activity towards PBMC culture as a non-aggregated form in solution.

The same measurements performed with dendrimer **D-2** (Figure 3) did not allow the identification of a clear plateau drop, and no CAC could be determined either from water or PBS solutions at concentrations lower than 10^{-1} mol.L^{-1}. This result shows that dendrimer **D-2** is not present in cell cultures as aggregated species. Thereby the cytotoxicity of dendrimer **D-2** cannot be attributed to any detergent effect of the amphiphilic dendrimer. Interestingly, the biological difference between monocyte activating dendrimer **D-1** and non-activating compound **D-2** can be correlated to differences in the physicochemical behaviour, which are due only to structural differences affecting solely the chemical nature of the surface functions. Dynamic Light Scattering (DLS) experiments on water and PBS solutions of dendrimers **D-1** and **D-2** did not provide treatable information. Actually, signals with very low intensities were observed, even above the CAC values, meaning that small aggregates formed in solution and/or the concentration of aggregates was very low.

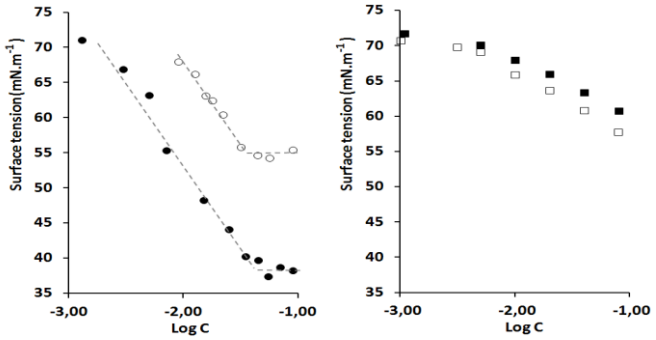

Figure 3. Tensiometry of **D-1** (left) and **D-2** (right) in water (plain) and PBS solution (hollow).

In a second step, we have explored the interactions between PPH dendrimers and DPPC (dipalmitoylphosphatidylcholine) monolayers, used as 2D models of biological membrane. The compression isotherms and the monolayer morphologies observed by Brewster Angle Microscopy (BAM) were used to evaluate the possible incorporation of dendrimers **D-1** and **D-2** from a PBS subphase into a DPPC monolayer.[25,26] Compression isotherms (Figure 4) were first obtained to investigate modifications induced in the behaviour of DPPC monolayers[21] by the migration of dendrimer **D-1** and **D-2** from the subphase bulk to the surface. During the compression of the surface, the relative pressure was recorded as a function of area per DPPC molecule and the morphology of the surface was monitored through BAM.

For PBS subphase, compression was run 15 min after DPPC deposition, while for dendrimer subphases determination of isotherm curve directly followed the achievement of an equilibrium pressure on the surface.[21] While the phospholipid film was compressed with a speed of 1,2 $Å^2.molecule^{-1}.min^{-1}$ (7 $cm^2.min^{-1}$), an initial equilibrium pressure of 3-4 $mN.m^{-1}$ was reached in both cases, revealing a weak but not negligible incorporation of dendrimers in monolayer's expanded phase. In addition, DPPC-dendrimers (PBS solutions) isotherms showed higher pressure values than DPPC-PBS isotherm up to 50 and 45 $Å^2.molecule^{-1}$ for **D-1** and **D-2** respectively, revealing the presence of dendrimer molecules inside the monolayers until pressures of about 55 $mN.m^{-1}$, at which **D-1** and **D-2** were probably squeezed out from the monolayers. In the case of **D-1** the compression profile resembles the one observed for DPPC-PBS isotherm (even if the typical zone of expanded liquid phase is not visible). On the contrary, the compression profile observed with **D-2** reaches a surface pressure of 40 $mN.m^{-1}$ for a specific molecular area of 95 $Å^2.molecule^{-1}$. This high lateral pressure obtained at high area values traduces a drastic modification of monolayer properties, induced by the insertion of **D-2** among phospholipids in the monolayer itself, whereas the incorporation of **D-1** in the monolayer does not seem to affect dramatically its properties.

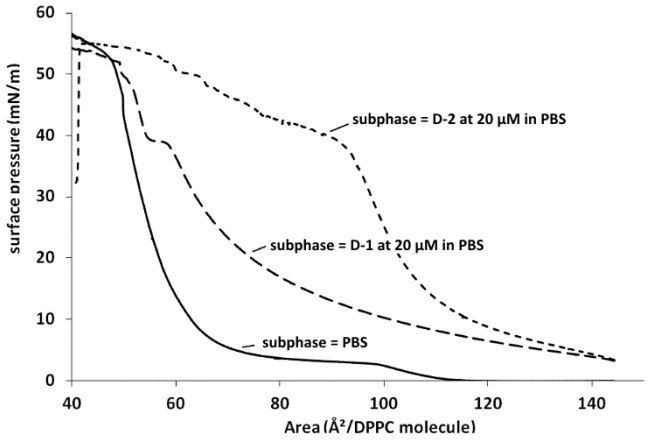

Figure 4. DPPC compression isotherms at 20 °C onto different subphases.

BAM images further confirmed these results. Actually, in presence of **D-1** in the subphase, liquid expanded phase observed for pure DPPC monolayer disappeared, to give way to typical large bright domains for DPPC monolayer (Figure 5), traducing liquid expanded-liquid condensed (LE-LC) phase transition, already detectable at 140 $Å^2.molecule^{-1}$. In addition, monolayer of DPPC in presence of **D-2** clearly showed the coexistence of two phases during the early stages of compression (Figure 4), characterized by round dark domains on bright background at 130 $Å^2.molecule^{-1}$. This suggests a major modification of the DPPC monolayer, where the two components are only partially miscible at the interface, with the coexistence of two phases during the compression. For both dendrimers, the monolayers of DPPC are modified, clearly indicating the interaction between the phospholipid and the dendrimers. In addition, dendrimer **D-2** seems to have stronger interactions with DPPC molecules, which could explain the dramatic modification of the compression profile of DPPC monolayers in the presence of a PBS subphase containing **D-2**.

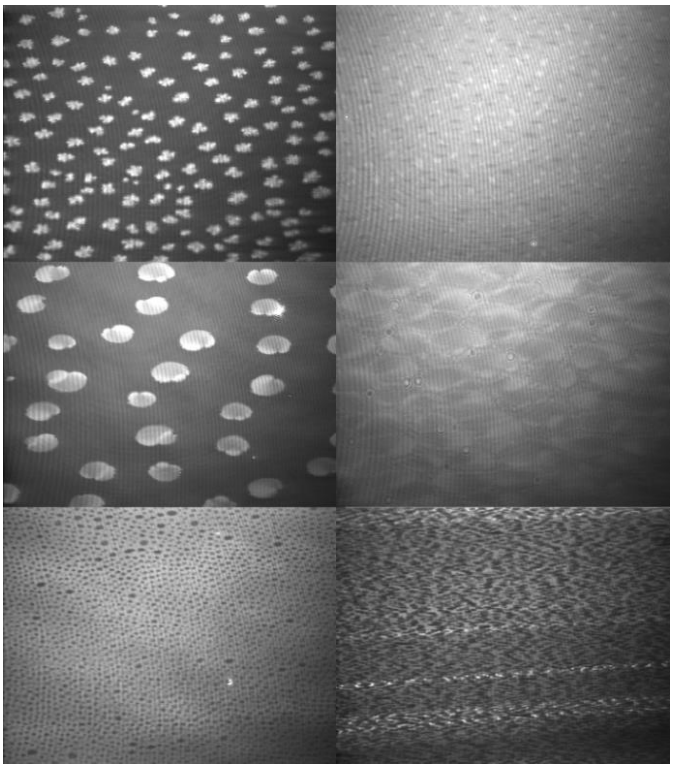

Figure 5. BAM images of DPPC monolayer, taken with 532 nm laser and 10X objective; from left to right, in the top row: DPPC on PBS at 64 and 50 $Å^2.molecule^{-1}$; in the middle row: DPPC on **D-1**-PBS at 140 and 50 $Å^2.molecule^{-1}$; in the bottom row: DPPC on **D-2**-PBS at 130 and 50 $Å^2.molecule^{-1}$.

The data retrieved from BAM technique unambiguously traduce the existence of strong interactions between **D-2** and DPPC molecules, as well as between **D-1** and DPPC, with fewer incidences on the DPPC monolayer properties. These interactions can find origin in lipophilic effects between phospholipids alkyl chains and dendrimers hydrophobic moieties as well as other weak interactions involving the dendrimer outershell and polar region of the DPPC. Nevertheless, whatever the dendrimer, both **D-1** and **D-2** remain inside the DPPC monolayer at pressures higher than 33 $mN.m^{-1}$ which corresponds to the average lateral pressure in biological membranes.[27] This point

seems to stand for the ability of both dendrimers to interact with phospholipidic cell membranes.

More information about the interactions with phospholipids was further expected from modifications in the thermotropic behaviour of DPPC bilayers in the presence of dendrimers **D-1** and **D-2** as measured by Differential Scanning Calorimetry (DSC).[24] In fact, DSC is a sensitive technique often used to probe bilayer alterations provoked by external molecules, as variations in the polar headgroups spacing or penetration into the lipophilic environment.[28] Thus, DPPC multi-lamellar vesicles (MLV) were used as a model of DPPC bilayer. To determine the DPPC concentration at which phospholipids' pre-transition and main transition peak are well detected, the experiment was first performed on pure DPPC suspensions. At 30 mM of DPPC in the sample, the pre-transition signal caused by conversion of bilayer's lamellar gel phase into a rippled gel phase, was found to be optimal. The main transition peak, corresponding to the transition from gel phase to a liquid crystal phase, was also well resolved. At the transition maximal temperatures (Tm) the endothermic ΔH values were registered. As previously determined with 30 mM DPPC samples,[20] the appropriate dendrimer/MLVs ratio was obtained with 10% molar ratio of dendrimer.

Table 1. Calorimetric data for DPPC suspension at 30 mM containing 10% of dendrimer **D-1** or **D-2**.

	Scan number	Main transition[a]		Early transition[a]	
		T_m (°C)	ΔH[b]	T_m (°C)	ΔH[b]
DPPC 30 mM	1st	42.7	6.6	36.5	0.9
	4th	42.9	6.6	36.5	1.0
DPPC 30 mM	1st	42.7	7.4	35.9	1.1
+ **D-1** 10%	4th	42.6	7.4	35.9	0.8
DPPC 30 mM	1st	42.7	7.2	36.4	0.9
+ **D-2** 10%	4th	42.5	4.8	35.9	0.4

[a] values are given for heating cycles. Cooling cycles gave comparable absolute values. [b] units: kcal/mol

Variations of thermodynamic features of pre-transition and main transition between the 1st and the 4th scan (Table 1, Figure 6) can be related to interactions between MLVs bilayer structures and dendrimers, as they generally traduce modifications in the extent of cooperativity of the DPPC molecules during the transitions.[29] Despite the low intensity and broad distribution of pretransition peaks a clear shift of maximal point towards lower temperatures and an intensity drop are observed in the presence of **D-2**. Pretransition signals are known to be very sensitive to the presence of external substances which can cause their disappearance at very low concentration. According to previous work, this disappearance can be related to dendrimer insertion into the bilayer, which increases the spacing between polar heads of DPPC and results in the absence of conversion of lamellar phase into rippled phase.[29] The insertion of perturbing molecule within the bilayer is also usually associated to a reduction of the cooperativity between DPPC molecules. This phenomenon, which is traduced by an increase of the peak width at half-height, is more pronounced in the presence of dendrimer **D-2**. Interestingly, the main transition peak seems also to be more affected by the presence of **D-2** than by the presence of **D-1**, despite small changes in the maximal temperatures (T_m). For instance, the relative enthalpic value is significantly lowered, while the peak width at half-height is increased, upon cycling in the presence of **D-2**. The signal broadening in the presence of **D-2** is accompanied by a loss of symmetry and skewing towards lower temperature which traduces a heterogeneous distribution of the dendrimer within the bilayer. This chaotic insertion can also lead to the formation of dendrimer-rich micro-domains resulting in the decrease of degree of order of the bilayer.

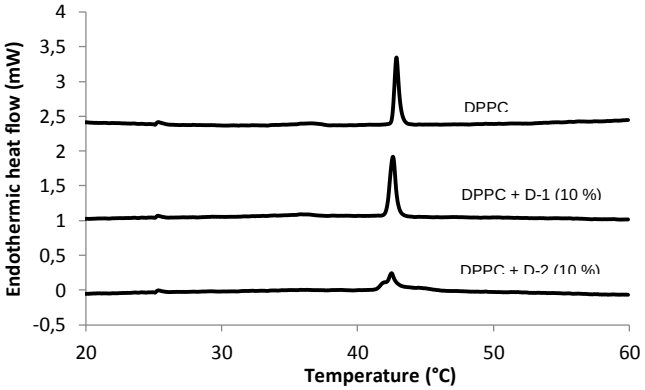

Figure 6. Influence of a 10% content of **D-1** and **D-2** on the thermograms of DPPC. All scans correspond to an equilibrium state after the fourth cycle.

These data show that interactions between **D-1** and DPPC bilayer are weaker than the one observed in the case of the dendrimer **D-2**. This observation suggests the existence of interactions with the hydrophobic phospholipids tails during all four heating/cooling cycle which are responsible for the reduction of cooperativity in the conversion of the gel phase to a liquid crystal phase in the case of dendrimer **D-2**. This modification of the phase transition peak could be explained by the fluidization of the gel phase of the DPPC membrane, as already described by Y.Q Ma and coll. with high generation PAMAM dendrimers.[30] We could expect that these dramatic changes in pure lipid bilayer physicochemical properties, would be observed in a more complex system, like a cell membrane. In fact it was already demonstrated that PAMAM dendrimers of high generation are more toxic because of their ability to modify the membrane structure and properties.[31,32] All these data comfort our assumption that the modification of cell functions in presence of dendrimer **D-2**, could be responsible for its toxicity observed on PBMC.

For the visualization of the interactions of a PPH dendrimer having carboxylate endgroups with the cell membrane of monocytes, a fluorescently labelled dendrimer **D-7**, analogue of dendrimer **D-2**, was designed (Scheme 1). The synthetic

approach is based on the modification of fluorescent dendrimer **D-3** equipped with a julolidine-based fluorescent tag on the cyclotriphosphazene ring and $PSCl_2$ surface functions.[15] The carboxylate surface functions are grafted by nucleophilic substitution of the terminal chlorine atoms with tert-butoxy-4-hydroxybenzoate in the presence of cesium carbonate in THF. Like for other PPH dendrimers, this transformation is monitored by ^{31}P NMR.[33] The dissymmetry originating at the core of the molecule gives rise on the ^{31}P NMR spectrum of the ter-butoxy-terminated intermediary dendrimer **D-5** to a broadening of the singlet corresponding to the branching thiophosphorus atoms at 61.9 ppm. Following ter-butoxy deprotection, the dissymmetry of the resulting polycarboxylic acid dendrimer **D-6** leads to the appearance on the 31P NMR spectrum of a set of two singlets at 61.9 and 62.5 ppm. On the ^{31}P NMR spectrum of compound **D-7** the dissymmetry is traduced by the presence of 3 singlets at 61.9, 62.0 and 63.5 ppm in 2:2:1 ratio which is coherent with the expected theoretical ratio.[34] The fact that dissymmetry is only fully traduced on ^{31}P NMR spectrum of the water-soluble compound **D-7** might possibly be related to its constraint structure in a mixture of solvents which could favour segregation of lipophilic and hydrophilic segments.

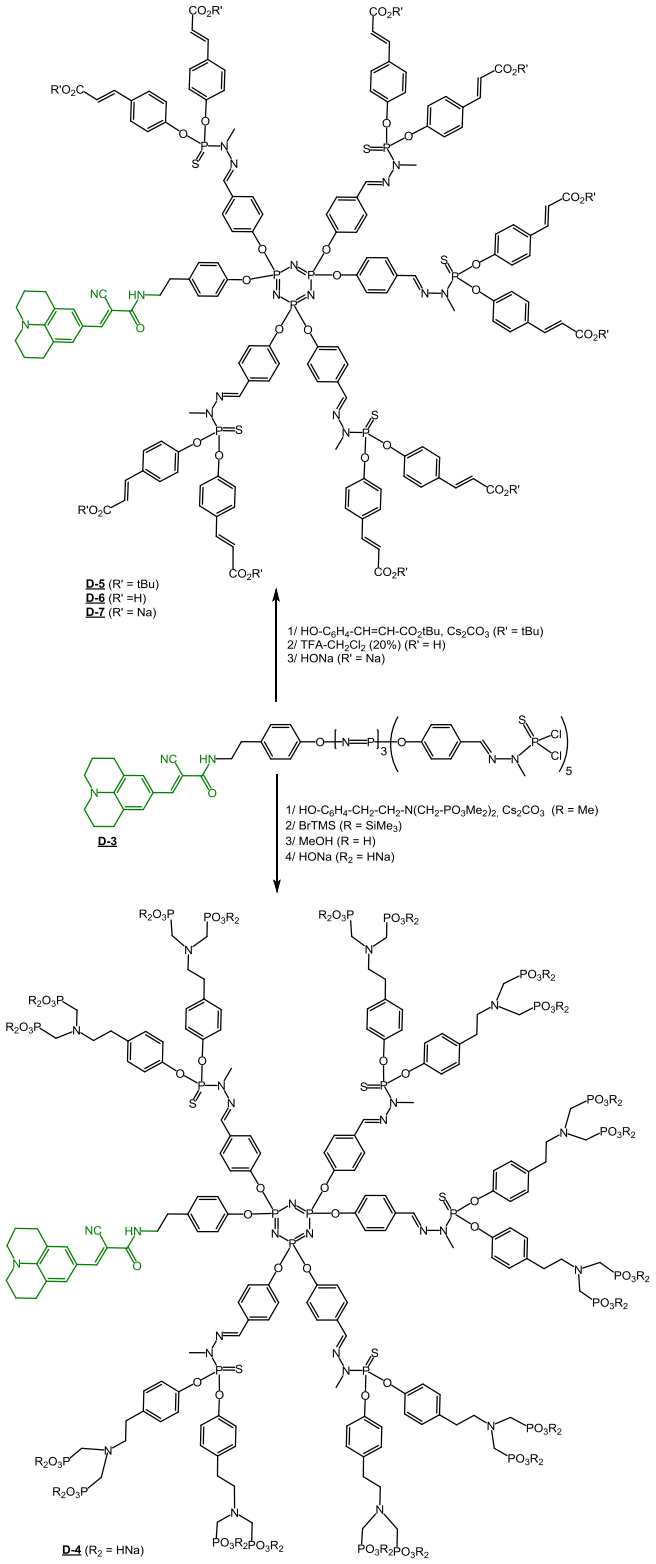

Scheme 1. Synthesis of fluorescent analogs **D-4** and **D-7**.

These fluorescent analogues of dendrimers **D-1** and **D-2** were used to correlate the difference of activity of both dendrimers towards the activation of human monocytes and their surface functions. Monocytes are white blood cells that play a pivotal role as a first line of defence in the organism, especially against infections and at the onset of inflammatory responses. They are also strongly involved in the resolution of inflammation as they are activated by anti-inflammatory signals and become in turn producers of anti-inflammatory mediators. At first, we have evaluated the bioactivity of fluorescent dendrimers **D-4** and **D-7** towards purified human monocytes in comparison with the lead dendrimer **D-1** by measuring the rate of activated monocytes in 3-4 days cultures by flow cytometry. This analysis is based on morphological criteria (Figure 7 and 8). Actually, activated monocytes are known to undergo morphological changes, namely an increase of their size and their granularity.[18] These morphological changes are also accompanied by phenotypical changes and modification of the physiological response.[11] Flow cytometry experiments were analysed with a polygonal gate enclosing all activated monocytes (Figure 7).

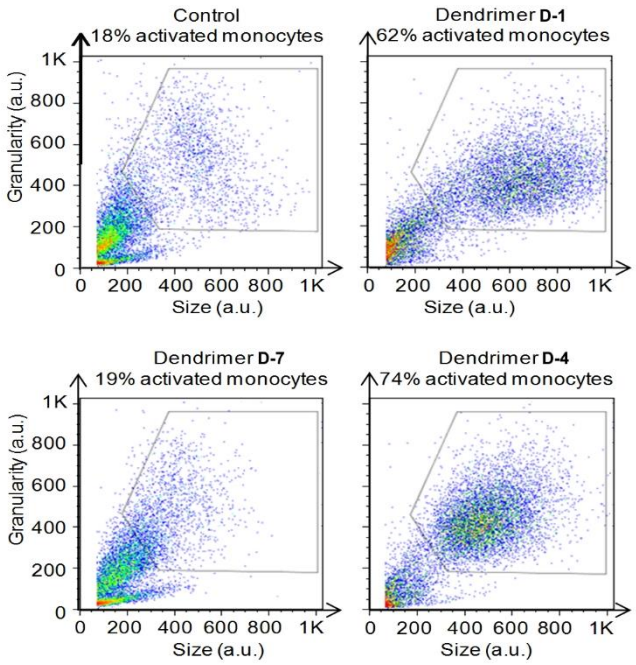

Figure 7. Flow cytometry-based morphological analysis of the percentage of activated human monocytes with dendrimers **D-1**, **D-4**, **D-7**.

Dendrimer **D-4** is as active as dendrimer **D-1**, both compounds lead to rates of activated monocytes of 62% and 74% respectively after 3 days of culture. On the contrary dendrimer **D-7** was found to be inactive, with a rate of activated monocytes at the same level than control monocytes cultured in the absence of dendrimers (Figure 7, positive control). The fact that dendrimer **D-7** is inactive is highly related to our previous findings showing the lack of activity of dendrimer **D-2**.[18] These results are confirmed by a clear dose-response effect (1 to 50 µM) which is observed for both active dendrimers **D-1** and **D-4** (Figure 8). For both molecules, activation of monocytes is detected at 5 µM and, as awaited, the maximum activity is reached at 20 µM. Dendrimer **D-7** is not active at all in the range of tested concentrations.

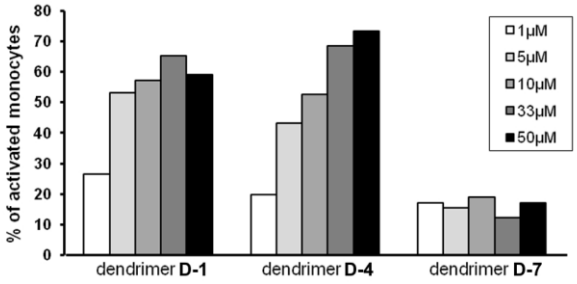

Figure 8. Dose dependent activation of human monocytes measured by the percentage of activated monocytes after 3 days of culture.

Then, fluorescent dendrimers **D-4** and **D-7** have been incubated with human monocytes. Incubation was performed at 4°C to avoid internalization of the molecules. The binding of these fluorescent analogues at the surface of monocytes has been revealed using confocal microscopy (Figure 9a). As expected, dendrimer **D-4** binds to the membrane of monocytes, but surprisingly dendrimer **D-7** also does. To compare the nature of the binding of dendrimers **D-4** and **D-7**, we have tested a range of concentrations and binding has been quantified using flow cytometry. Clearly, the binding of dendrimer **D-D-7** directly correlates to the concentration indicating a non-specific binding of the molecule (Figure 9b). Conversely, the binding of dendrimer **D-4** fits a logarithmic curve showing a saturation asymptote typical of a specific binding component. This indicates that surface receptor(s) are involved in the recognition of this molecule.

Therefore, the specific binding of acid phosphonic capped dendrimers on cell membrane of human monocytes and their activating properties towards these cells is dramatically correlated to the presence of aza-bisphosphonate groups at the surface of the dendritic inner shell. Conversely, carboxylate capped PPH dendrimers do not show specific binding on the cell membrane of human monocytes and do not either activate monocytes. These findings comfort previous results obtained with the strict analogue of dendrimer **D-1**, bearing twelve azabiscarboxylate groups, indicating that specific receptor(s) is (are) involved in the recognition and activation of human monocytes by PPH dendrimer **D-1**.[20]

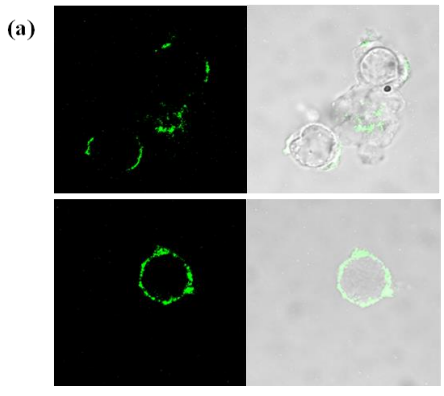

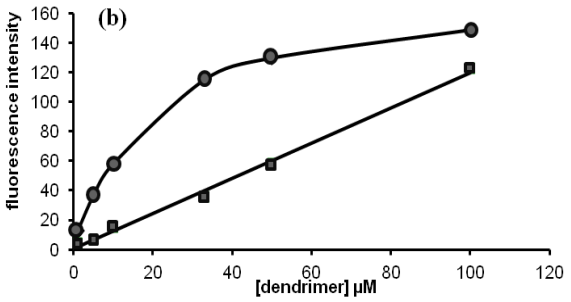

Figure 9. (a) confocal microscopy (left: fluorescence alone, right: fluorescence and phase contrast) of pure human monocytes incubated 30 min at 4°C with 50 µM of dendrimer **D-4** (top) or dendrimer **D-7** (bottom). (b) Binding curves of dendrimers **D-4** (dots) and **D-7** (squares) quantified by flow cytometry. One experiment representative of three.

Experimental Section

General procedures: Reactions were performed under inert atmosphere using vacuum-line manipulations and standard Schlenk techniques when carried out in organic solvents. All commercial samples were used as received without further purifications. All solvents were dried and/or distilled according to routine procedure. Thin layer chromatography was performed on Merck Kieselgel 60F254 precoated silicagel plates. Preparative chromatography was carried out on Merck Kieselgel. ^{1}H, ^{13}C, ^{31}P NMR, HMQC and HMBC measurements were performed on Bruker ARX 250, DPX 300, AMX 400 and Avance 500. Coupling constants are reported in Hertz (Hz) and chemical shifts in ppm/TMS for ^{1}H and ^{13}C. Chemical shifts for ^{31}P spectra are calibrated with phosphoric acid as an external reference. The first-order peak patterns are indicated as s (singlet), d (doublet), t (triplet), q (quadruplet), qn (quintuplet). Complex non-first-order signals are indicated as m (multiplet). ^{13}C NMR signals were assigned using HMQC and HMBC sequences when required. The numbering used for NMR assignment is showed on Figure 10. The following compounds have been prepared according to published procedures: julolidine-cored dendrimer **D-3**,[15] dendrimer **D-1**, dendrimer **D-2**,[35] dendrimer **D-4**.[15] The preparation of tert-butoxy-4-hydroxybenzoate was adapted from published procedures.[36]

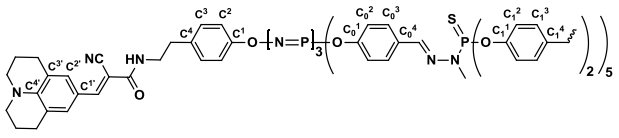

Figure 10. Numbering scheme for NMR assignment.

Synthesis of dendrimer D-5: To a solution of dendrimer **D-3** (203 mg, 0.105 mmol) and tert-butoxy-4-hydroxybenzoate (255 mg, 1.159 mmol) in THF (6.5 mL) maintained at 0°C, cesium carbonate is added (752 mg, 2.310 mmol in 4 portions). The reaction mixture is then stirred at RT for 12 hours, centrifuged and then filtered. The resulting solution is evaporated to dryness under reduced pressure. The crude residue is purified by column chromatography (hexane/AcOEt, 4:1 to 1:1, Rf (hexane/AcOEt, 2:1) = 0.17) to yield dendrimer **D-5** as yellow powder (331 mg, 87%). $^{31}P\{^{1}H\}$ NMR ($CDCl_3$, 121.5 MHz): δ = 8.4 (s, N_3P_3); 61.9 (m, P=S); ^{1}H NMR ($CDCl_3$, 300.1 MHz): δ = 1.52 (s, 90H, $C(CH_3)_3$); 1.56 (br s, 4H, CH_2-C$\underline{H_2}$-CH_2-N); 1.90-2.00 (m, 4H, C$\underline{H_2}$-CH_2-CH_2-N); 2.60-2.80 (m, 6H, CH_2-CH_2-C$\underline{H_2}$-N and C$\underline{H_2}$-CH_2-NH); 3.26-3.35 (m, 15H, NCH_3); 3.40-3.55 (m, 2H, CH_2-C$\underline{H_2}$-NH); 6.25 (d, $^{3}J_{HH}$ = 15.9 Hz, 10H, CHCO); 6.70-6.80 (m, 2H, C^2H); 6.90-7.10 (m, 14H, $C_0{}^2H$, $C^{2'}H$ and C^3H); 7.16-7.21 (m, 20H, $C_1{}^2H$); 7.41 (br s, 20H, $C_1{}^3H$); 7.46 (d, $^{3}J_{HH}$ = 15.9 Hz, 10H, Ar-C$\underline{H}$); 7.61-7.67 (m, 16H, $C_0{}^3H$, CH=N and HC=C-CN); $^{13}C\{^{1}H\}$ NMR ($CDCl_3$, 75.5 MHz): δ = 21.2 (br s, CH_2-C$\underline{H_2}$-CH_2-N); 27.6 (s, C$\underline{H_2}$-CH_2-CH_2-N); 28.2 (s, C($\underline{C}H_3)_3$); 32.8-33.0 (m, NCH_3); 34.2 (s, C$\underline{H_2}$-CH_2-NH); 41.0 (s, CH_2-C$\underline{H_2}$-NH); 50.1 (s, CH_2-CH_2-C$\underline{H_2}$-N); 80.6 (s, $\underline{C}(CH_3)_3$); 93.3 (s, $\underline{C}$-CN); 118.4 (s, CN); 120.4 (s, $\underline{C}$HCO); 120.7 (s, $C^{3'}$); 121.1 (s, C^2); 121.4 (s, $C_0{}^2$); 121.8 (s, $C_1{}^2$); 128.3 (s, $C_0{}^3$); 129.3 (s, $C_1{}^3$); 129.8 (s, C^3); 131.1 (s, $C^{2'}$); 131.3 (s, $C^{1'}$); 131.9 (s, $C_0{}^4$); 132.1 (s, $C_1{}^4$); 135.8 (s, C^4); 139.0 (br s, CH=N); 142.2 (s, Ar-$\underline{C}$H); 147.0 (s, $C^{4'}$); 151.6 (br s, $C_0{}^1$, $C_1{}^1$ and C^1); 152.2 (s, H$\underline{C}$=C-CN); 162.5 (s, CONH); 166.1 (s, $\underline{C}OO^tBu$) ppm.

Synthesis of dendrimer D-6: A solution of TFA in CH_2Cl_2 (20%, 20 mL) is added to a concentrated solution of dendrimer **D-5** (300 mg, 0.083 mmol) in CH_2Cl_2 (20%, 3 mL). The resulting solution is stirred at RT for 1.5 hours and then evaporated to dryness. *the crude residue is diluted with 5 mL of AcOEt and the resulting solution is evaporated to dryness under reduced pressure. This procedure is repeated until complete disappearance of TFA signal on ^{19}F NMR spectra to yield dendrimer **D-6** as a white powder. $^{31}P\{^{1}H\}$ NMR (d_6DMSO, 121.5 MHz): δ = 8.5 (s, N_3P_3); 61.9 (br s, P=S); 63.5 (s, P=S); ^{1}H NMR (d_6DMSO, 400.1 MHz): δ = 1.45-1.55 (m, 4H, CH_2-C$\underline{H_2}$-CH_2-N); 2.60-2.85 (m, 6H, C$\underline{H_2}$-CH_2-CH_2-N and C$\underline{H_2}$-CH_2-NH); 3.20-3.33 (m, 21H, NCH_3, CH_2-C$\underline{H_2}$-NH and CH_2-CH_2-C$\underline{H_2}$-N); 6.42 (d, $^{3}J_{HH}$ = 15.6 Hz, 10H, CHCO); 6.80-7.40 (m, 36H, C^2H, $C_0{}^2H$, $C^{2'}H$, C^3H and $C_1{}^2H$); 7.45-8.00 (m, 36H, Ar-C$\underline{H}$, $C_1{}^3H$, $C_0{}^3H$, CH=N and HC=C-CN); $^{13}C\{^{1}H\}$ NMR (d_6DMSO, 100.6 MHz): δ = 22.5 (s, CH_2-C$\underline{H_2}$-CH_2-N); 26.8 (s, C$\underline{H_2}$-CH_2-CH_2-N); 33.3 (br s, NCH_3); 34.1 (s, C$\underline{H_2}$-CH_2-NH); 41.6 (s, CH_2-C$\underline{H_2}$-NH); 49.5 (s, CH_2-CH_2-C$\underline{H_2}$-N); 93.0 (s, $\underline{C}$-CN); 117.4 (s, CN); 119.8 (s, CHCO); 120.9 (s, $C^{3'}$); 121.4 (s, $C_0{}^2$ and C^2); 121.9 (s, $C_1{}^2$); 128.7 (s, $C_0{}^3$); 130.2 (s, $C_1{}^3$); 130.5 (s, C^3); 131.7 (s, $C^{2'}$); 131.8 (s, $C^{1'}$); 132.2 (s, $C_1{}^4$); 132.4 (s, $C_0{}^4$); 137.0 (s, C^4); 141.0 (br s, CH=N); 143.1 (s, Ar-$\underline{C}$H); 143.2 (s, $C^{4'}$); 148.5 (br s, C^1); 150.5 (br s, $C_0{}^1$); 151.7 (br s, H$\underline{C}$=C-CN and $C_1{}^1$); 167.8 (s, COOH); 167.9 (s, CONH) ppm.

Synthesis of dendrimer D-7: An aqueous solution of sodium hydroxide (0.1023 N, 3.18 mL) is added dropwise to a suspension of dendrimer **D-6** (100 mg, 0.032 mmol) in water (5 mL) at 0°C. The resulting solution is filtered on micropore (1.2 µm) and freeze dried to yield dendrimer **D-7** as a white powder (102 mg, 97%). $^{31}P\{^{1}H\}$ NMR (D_2O/CD_3CN, 3:1, 121.5 MHz): δ = 8.5 (s, N_3P_3); 61.9 (s, P=S); 62.0 (s, P=S); 63.5 (s, P=S); ^{1}H NMR (D_2O/CD_3CN, 3:1, 300.1 MHz): δ = 1.70-1.80 (m, 4H, CH_2-C$\underline{H_2}$-CH_2-N); 2.30-2.65 (m, 6H, C$\underline{H_2}$-CH_2-NH and C$\underline{H_2}$-CH_2-CH_2-N); 3.18-3.27 (m, 15H, NCH_3); 3.50-3.90 (m, 6H, CH_2-C$\underline{H_2}$-NH and CH_2-CH_2-C$\underline{H_2}$-N); 6.34 (d, $^{3}J_{HH}$ = 15.0 Hz, 10H, CHCO); 6.65-6.75 (m, 2H, C^2H); 6.80-6.85 (m, 2H, $C^{2'}H$); 6.90-7.00 (m, 10H,

C_0^2H); 7.05-7.10 (m, 20H, C_1^2H); 7.22-7.25 (m, 2H, C^3H); 7.43 (d, $^3J_{HH}$ = 18.0 Hz, 10H, Ar-CH); 7.50-7.65 (m, 30H, C_1^3H and C_0^3H); 7.70-7.90 (m, 2H, CH=N and HC=C-CN): $^{13}C\{^1H\}$ NMR (D_2O/CD_3CN, 3:1, 75.5 MHz): δ = 22.1 (s, CH_2-CH_2-CH_2-N); 27.0 (s, CH_2-CH_2-CH_2-N); 32.9 (br s, NCH_3); 35.1 (s, CH_2-CH_2-NH); 40.3 (s, CH_2-CH_2-NH); 49.2 (s, CH_2-CH_2-CH_2-N); 93.9 (s, C-CN); 117.5 (s, CN); 119.3 (s, CHCO); 120.3 (s, $C^{3'}$); 120.8 (s, C_0^2 and C^2); 121.3 (s, C_1^2); 128.2 (s, C_0^3); 129.7 (s, C_1^3); 130.1 (s, C^3); 131.7 (s, $C^{2'}$); 131.9 (s, $C^{1'}$); 134.0 (s, C_1^4); 135.0 (s, C_0^4); 138.0 (s, C^4); 140.0 (br s, CH=N); 142.6 (s, Ar-CH); 143.5 (s, $C^{4'}$); 147.5 (br s, C^1); 151.1 (s, C_0^1); 151.2 (s, HC=C-CN and C_1^1); 167.4 (s, CONH); 174.7 (s, COONa) ppm.

Tensiometry: Surface tension measurements were performed using a tensiometer from Kruss, GmbH (Germany) on aqueous and PBS buffer solutions of dendrimers **D-1** and **D-2**, in order to calculate their critical aggregation concentration (CAC). The "pendant drop" method was used for all the measurements. The profile of a pendant drop, suspended from a needle in air is analyzed by means of optical methods to determine the surface tension of a solution. The surface tension between the inner and outer phases results in an increased pressure inside the drop. The surface tension is then determined using the equation of Young-Laplace, that correlates this difference in pressure to the radii of curvature of the surface and the interfacial tension [$\Delta p = \sigma (1/r_1+1/r_2)$]. Surface tension values obtained at 20°C with the Drop Shape Analysis software, were graphically plotted versus the logarithm of the corresponding sample concentrations; CACs were then extrapolated from the graphs obtained.

Monolayer experiments: Isotherms were obtained with a NIMA trough (type 601BAM) (BAM = Brewster Angle Microscopy) equipped with a Wilhelmy plate and maintained at constant temperature of 20°C. A BAM2plus from NFT was used for the Brewster angle microscopy experiments. BAM apparatus was equipped with a 532 nm laser and a 10X objective. The trough was filled with PBS, or a PBS solution of **D-1** or **D-2** (20 µM), then the system temperature set up on 20°C; the spreading of a little amount of a 2 mM chloroform solution of 1,2-dipalmitoyl-sn-glycero-3-phosphocholine (DPPC) onto the surface, previously cleaned with a water pump, led to monolayer formation (144 $Å^2$/DPPC molecule with open barriers). During compression experiments, surface pressure was recorded as a function of area per DPPC molecule and the morphology of the surface was monitored through BAM; for PBS only subphase, compression was run immediately after 15 min from DPPC deposition, while for PBS-dendrimer subphases determination of compression isotherm curve directly followed the achievement of an equilibrium pressure on the surface; in every case, trough barriers were closed and the phospholipids film compressed with a speed of 1.2 $Å^2$. $molecule^{-1}$. min^{-1}.

Multi-Lamellar Vesicles: MLVs were prepared according to an already described procedure.[37] After dissolution of DPPC in pure $CHCl_3$, the solvent is evaporated to dryness under reduced pressure at room temperature. The resulting phospholipids dried film is then rehydrated with a solution of PBS and kept for 20 minutes above the main transition temperature (52°C). The suspension is then stored at 4°C.

Differential Scanning Calorimetry: The resulting MLV suspension is diluted to obtain a final concentration in DPPC of 30 mM, with PBS (to record thermograms of pure DPPC vesicles) or with dendrimer solutions (to study DPPC-dendrimer systems). All analyses were completed with a Perkin-Elmer Differential Scanning Calorimeter, in a temperature range between 10°C and 60°C. All experiments are realized on 30 µL of DPPC suspension and dendrimer-DPPC mixtures at 10% molar ratio. Samples are put in aluminum crucibles, sealed with tap; an empty one is used as blank. Six heating/cooling cycles are programmed. The first two at a scanning rate of 20°/min and 10°/min (sample equilibration) and the following four at a rate of 1°/min. Between heating/cooling cycles, isothermic steps of 10 min at 10°C are also programmed. Thermograms and calorimetric data were determined with the Perkin Elmer "Pyris Series" software.

PBMC purification: Fresh blood samples were collected from healthy adult donors, PBMC were isolated on a Ficoll-Paque density gradient (Amersham Biosciences AB, Upsalla, Sweden) and diluted at 1.5 million cells per mL in complete RPMI 1640 medium supplemented with penicillin / streptomycin (100 U per mL) (Cambrex Bio Science, Verviers, Belgium), 1 mM sodium pyruvate and 10% heat-inactivated fetal calf serum (both from Invitrogen Corporation, Paisley, UK)

PBMCs viability assay: PBMCs freshly purified from 5 donors were resuspended in a 96-well plate round u bottom for 1 and 3 days at 37°C at 1.5 million cells/ml in complete RPMI 1640 medium. All molecules were added at the beginning of the cultures at the specified concentrations (0.2; 2; 20; 200 µM), with H_2O or with staurosporine (STS) (Sigma-Aldrich, Saint-Louis, Mo, USA) at 0.5 µM (positive control of cytotoxicity). Cell viability was quantified by CellTox™ Green Cytotoxicity Assay (Promega, Madison, WI, USA) protocol. PBMCs were divided into two volumes in 96-well black, one was treated with 2X volume of CellTox™ Green Dye which binds DNA of cells with impaired membrane integrity. The other one was used like an autofluorescence control due to certain dendrimers. Fluorescence was measured using the Varioskan™ Flash Multimode Reader (Thermo Fisher Scientific Inc, Waltham, MA, USA). Cytotoxicity ratio was calculated using the following formula:

Cytotoxicity fluorescence = (fluorescence treated sample – autofluorescence sample)

Cytotoxicity ratio = Cytotoxicity fluorescence / STS fluorescence

Monocyte purification and culture: Monocytes were purified from freshly isolated PBMCs by negative selection, according to the manufacturer's instructions (Dynabeads Untouched Human Monocytes, Invitrogen Dynal AS, Oslo, Norway). Purity of the monocytes was assessed by flow cytometry using a FACS-Scan cytometer (BD Biosciences, San Jose, CA, USA) and cells were > 98% pure.

Bioactivity of dendrimers: 3.10^5 monocytes were cultured for 72 to 96 hr in 200 µL of complete RPMI 1640 medium in a 96-well plate. At the beginning of the cultures, dendrimers **D-1** (positive control), **D-4** or **D-7** were added at the specified concentration, between 1 and 50 µM. Activation of the monocytes, assessed by morphological

changes, was analyzed by flow cytometry using a FACS-Scan cytometer. A polygonal gate was created to quantify the rate of activated monocytes.

Binding of fluorescent dendrimers on monocyte cell surface: Highly pure monocytes were incubated with dendrimers **D-4** or **D-7** at the specified concentrations, at 4°C for 30 min. Binding was analyzed either by confocal microscopy or by flow cytometry (FACS Scan device). A LSM 510 confocal microscope (Carl Zeiss, Iena, Germany) was used with the 63X lense (ON 1.4 Plan-Apo) with a (x2) numeric zoom. Images were performed with the LSM Image Browser software.

Conclusions

Following an essentially physicochemical approach, which included various experimental techniques and different cell membrane models, we have shown several differences in the way dendrimer **D-1** and **D-2** interact with biologically relevant membrane models. Both dendrimers revealed, in physiologic conditions, to be capable, although with different extents, to interact with phospholipid molecules. Interestingly, the monocyte activating dendrimer **D-1** has a lower impact on phospholipidic monolayers and bilayers having physical characteristics close to the ones of a cell membrane. Indeed, only dendrimer **D-2** strongly disturbs and alters the structure and the properties of the studied models, explaining the cytotoxicity of this specific dendrimer. Taking into account that previous Molecular Modelling studies studies[20] have shown that carboxylates penetrate more deeply in bilayer model membranes, a tentative assumption could be that less hindered cinnamate terminations on dendrimer **D-2** allow a more compact conformation that could possibly penetrate deeper and more easily in the bilayer membrane, enhancing it perturbating properties.

This observation also represents a substantial clue for a specific, receptor(s)-mediated, mechanism for the adhesion-internalisation-activation process of dendrimer **D-1** and fluorescent analogues in monocytes.[20] The fact that dendrimer **D-1** adheres only to monocytes in the very first minutes of PBMC (Peripheral Blood Mononuclear Cells) cultures is actually striking. The fact that lymphocytes and monocytes have similar phospholipidic membrane fractions, with slight differences in the cholesteric content,[38] also supports to a certain extent the involvement of a receptor or of a pool of receptors on the surface of monocytes. This first step would then be followed by a safe incorporation into the monocyte membrane and subsequent endosome-lysosome cytoplasmic release.[18] In this regard, we are currently trying to identify potential receptors involved in this monocyte-activating process.

Acknowledgements

CNRS, INSERM, and University Paul Sabatier of Toulouse are acknowledged for institutional funding. We thank Sophie Allart for technical assistance at the cellular imaging facility of INSERM 1043, Toulouse. This research work was supported by the European Community (F. Ielasi and A. Perez-Anes, Marie Curie EST "Nanotool") and by the French Fondation pour la Recherche Médicale" (J. Ledall, "Chemistry for Medicine" project DCM20111223039).

Notes and references

1 Dendrimers: Towards Catalytic, Material, Biomedical Uses (Eds A.-M. Caminade, C.-O. Turrin, R. Laurent, A. Ouali, B. Delavaux-Nicot), John Wiley & Sons, Ltd, Chichester, UK, 2011.
2 O. Rolland, C.-O. Turrin, A.M. Caminade, J.P. Majoral, *New J. Chem.*, 2009, **33**, 1809.
3 N. Launay, A.M. Caminade, J.P. Majoral, *J. Organomet. Chem.*, 1997, **529**, 51.
4 A.M. Caminade, J.P. Majoral, *Prog. Polym. Sci.*, 2005, **30**, 491.
5 M. Mammen, S. K. Choi, G. M. Whitesides, *Angew. Chem. Int. Ed.*, 1998, **37**, 2754.
6 A. Pérez-Anes, C. Stefaniu-Bololoï, C. Moog, J.-P. Majoral, I. Rico-Lattes, M. Blanzat, A.-M. Caminade, C.-O. Turrin, *Bioorg. Med. Chem.*, 2010, **18**, 242.
7 A.M. Caminade, C.-O. Turrin, J.P. Majoral, *Chem. Eur. J.*, 2008, **14**, 7422.
8 Bouchara, L. Rozes, G. J. D. Soler-Illia, C. Sanchez, C. O. Turrin, A. M. Caminade, J. P. Majoral, *J. Sol-Gel Sci. Tech*., 2003, **26**, 629.
9 A. Pérez-Anes, G. Spataro, Y. Coppel, C. Moog, M. Blanzat, C. O. Turrin, A. M. Caminade, I. Rico-Lattes, J. P. Majoral, *Org. Biomol. Chem.*, 2009, **7**, 3491.
10 L. Griffe, M. Poupot, P. Marchand, A. Maraval, C.-O. Turrin, O. Rolland, P. Metivier, G. Bacquet, J. J. Fournie, A. M. Caminade, R. Poupot, J. P. Majoral, *Angew. Chem. Int. Ed.*, 2007, **46**, 2523.
11 S. Fruchon, M. Poupot, L. Martinet, C. O. Turrin, J. P. Majoral, J. J. Fournie, A. M. Caminade, R. Poupot, *J. Leukoc. Biol.*, 2009, **85**, 553.
12 D. Portevin, M. Poupot, O. Rolland, C.-O. Turrin, J.-J. Fournié, J.-P. Majoral, A.-M. Caminade, R. Poupot, *J. Trans. Med.*, 2009, **7**, 82.
13 M. Hayder, M. Poupot, M. Baron, D. Nigon, C.-O. Turrin, A.-M. Caminade, J.-P. Majoral, R.A. Eisenberg, J.-J. Fournié, A. Cantagrel, R. Poupot, J.-L. Davignon *Sci. Transl. Med.*, 2011, **3**, 81ra35. doi: 10.1126/scitranslmed.3002212.
14 M. Hayder, M. Varilh, C.-O. Turrin, A. Saoudi, A.-M. Caminade, R. Poupot, R.S. Liblau *Biomacromolecules*, 2015, **16**, 3425.
15 O. Rolland, L. Griffe, M. Poupot, A. Maraval, A. Ouali, Y. Coppel, J. J. Fournié, G. Bacquet, C. O. Turrin, A. M. Caminade, J. P. Majoral, R. Poupot, *Chem. Eur. J.*, 2008, **14**, 4836.
16 P. Marchand, L. Griffe, M. Poupot, C. O. Turrin, G. Bacquet, J. J. Fournie, J. P. Majoral, R. Poupot, A. M. Caminade, *Bioorg. Med. Chem. Lett.*, 2009, **19**, 3963.
17 A.M. Caminade, S. Fruchon, C.O. Turrin, M. Poupot, A. Ouali, A. Maraval, M. Garzoni, M. Maly, V. Furer, V. Kovalenko, J.P. Majoral, G. M. Pavan, R. Poupot, *Nat Commun*, 2015, **6**, 7722.
18 M. Poupot, L. Griffe, P. Marchand, A. Maraval, O. Rolland, L. Martinet, F. E. L'Faqihi-Olive, C. O. Turrin, A. M. Caminade, J. J. Fournie, J. P. Majoral, R. Poupot, *FASEB J.*, 2006, **20**, 2339.
19 O. Rolland, C. O. Turrin, G. Bacquet, R. Poupot, M. Poupot, A. M. Caminade, J. P. Majoral, *Tetrahedron Lett.*, 2009, **50**, 2078.
20 J. Ledall, S. Fruchon, M. Garzoni, G. M. Pavan, A. M. Caminade, C. O. Turrin, M. Blanzat, R. Poupot, *Nanoscale*, 2015, **7**, 17672.
21 A. Brun, G. Brezesinski, H. Möhwald, M. Blanzat, E. Perez, I. Rico-Lattes, *Colloids, Surfaces A: Physicochem. Eng. Aspects*, 2003, **228,** 3.
22 J. C. Garrigues, I. Rico-Lattes, E. Perez, A. Lattes, *Langmuir*, 1998, **14**, 5968.
23 C.V. Teixeira, M. Blanzat, J. Koetz, I. Rico-Lattes, G. Brezesinski, *Biochimica et Biophysica Acta*, 2006, **1758**, 1797.
24 C. Mestres, M. A. Alsina, M. A. Busquets, I. Haro, F. Reig, *Langmuir*, 1994, **10**, 767.

25 H. Zhang, X. Wang, G. Cui, J. Li, *Colloids, Surfaces A: Physicochem. Eng. Aspects*, 2000, **175**, 77.
26 E. Soussan, M. Blanzat, I. Rico-Lattes, A. Brun, C. V. Teixeira, G. Brezesinski, F. Al-Ali, A. Banu, M. Tanaka, *Colloids, Surfaces A: Physicochem. Eng. Aspects*, 2007, **303,** 55.
27 The membranes of cells, Third Edition (Ed. P. L. Yeagle) Academic Press, 2016.
28 K. Gardikis, S. Hatziantoniou, K. Viras, M. Wagner, C. Demetzos, *Int. J. Pharm.*, 2006, **318**, 118.
29 B. Klajnert, R.M. Epand, *Int. J. Pharm.*, 2005, **305**, 154.
30 L.Q. Xie, J.W. Feng, W.D. Tian, Y.Q. Ma, *Macomol. Theory Simul.*, 2014, **23**, 531.
31 H. Lee, R.G. Larson, *J. Phys. Chem. B*, 2006**, 110***,* 18204.
32 W.D. Tian, Y.Q. Ma, *Chem. Soc. Rev.*, 2013, **42**, 705.
33 A. M. Caminade, R. Laurent, C. O. Turrin, C. Rebout, B. Delavaux-Nicot, A. Ouali, M. Zablocka, J. P. Majoral, *C. R. Chim.*, 2010, **13**, 1006.
34 D. Riegert, A. Pla-Quintana, S. Fuchs, R. Laurent, C. O. Turrin, C. Duhayon, J. P. Majoral, A. Chaumonnot and A. M. Caminade*, Eur. J. Org. Chem.*, 2013, **24**, 5414.
35 M. Blanzat, C. O. Turrin, A. M. Aubertin, C. Couturier-Vidal, A. M. Caminade, J. P. Majoral, I. Rico-Lattes, A. Lattes, *ChemBioChem*, 2005, **6**, 2207.
36 S. W. Wright, D. L. Hageman, A.S. Wright, L. D. McClure, *Tet. Lett.*, 1997, **38**, 7345.
37 B. Klajnert, J. Janiszewska, Z. Urbanczyk-Lipkowska, M. Bryszewska, R.M. Epand, *Int. J. Pharm.*, 2006, **327**, 145.
38 K. Leidl, G. Liebisch, D. Richter, G. Schmitz, *Biochim. Biophys. Acta (BBA) - Molecular, Cell Biology of Lipids*, 2008, **1781**, 655.

